Research Papers

GREENSUSMATER

Greensusmater
Vol. 1, No. 1, March 2024
https://doi.org/10.62755/greensusmater.2024.1.1.15-19
Check for updates

Using hand painting in the fabrication of a negative refractive index metamaterial based on circular shape with paper as the dielectric

Felix R.M. Hamonangan M[1] Hadi Teguh Yudistira[1,2,3,] Fitrah Qalbina[1] Adhitya Gandaryus Saputro[4,5,] Amir Faisal[4,5,]

[1] Mechanical Engineering Study Program, Institut Teknologi Sumatera (ITERA), South Lampung, Lampung, 35365, Indonesia
[2] Research and Innovation Center for Conservation and Renewable Energy, Institut Teknologi Sumatera (ITERA), South Lampung, Lampung, 35365, Indonesia
[3] Research and Innovation Center for Advanced Materials, Institut Teknologi Sumatera (ITERA), South Lampung, Lampung, 35365, Indonesia
[4] Research Group of Advanced Functional Materials, Faculty of Industrial Technology, Institut Teknologi Bandung, Bandung 40132, Indonesia
[5] Research Center for Nanoscience and Nanotechnology, Institut Teknologi Bandung, Bandung, 40132, Indonesia
[6] Biomedical Engineering Study Program, Institut Teknologi Sumatera (ITERA), South Lampung, Lampung, 35365, Indonesia

Corresponding author: yudistira@ms.itera.ac.id

ARTICLE HISTORY: Received: February 13, 2024 | Revised: March 1, 2024 | Accepted: March 1, 2024

ABSTRACT

This study aims to use the hand-painting method in designing and fabricating a metamaterial based on a circular shape that exhibits a negative refractive index over the microwave spectrum. Hand painting is a simple and inexpensive fabrication method. This study applies silver ink as a periodic conductor to glossy paper as the dielectric substrate. The spectrum of investigation in this study is 3–6 GHz, and the experiment results are compared with the simulation results. The slight error obtained between transmission results from the simulation and the experiments reflects limitations in the fabrication methods used. Overall, the experiment results have a similar trend to the simulation results. The electrical properties of the metamaterial are retrieved from the transmission and reflection simulation results. The simulation results are employed instead of the experimental results because of the fluctuating data provided by the latter. The refractive index presents a negative value at 3–3.6 GHz

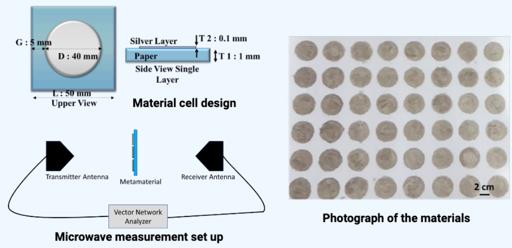

Keywords: *Electrical Properties, Hand Painting, Metamaterial, Negative Refractive Index, Circular*

1. INTRODUCTION

Metamaterials are synthetic materials tailoring electromagnetic properties that are challenging to obtain in nature. Metamaterials have attracted broad interest and have led to many potential electromagnetic applications, from microwaves to optical regimes. These applications reflect the unique characteristics of metamaterials, such as the ability to tailor electromagnetic properties [1]. Metamaterials are widely used in optics, especially as researchers seek to increase the image resolution of lenses by adjusting negative refractive index values [2, 3]. Besides being used in perfect lenses, metamaterials are also widely applied as biosensor metamaterials [4, 5], perfect absorbers [6, 7], intelligent surfaces [8], and high refractive index materials [9, 10]. The use of metamaterials is also highly developed in the field of aeronautics, especially in radar and the camouflaging of aircraft. With the addition of metamaterials to the fuselage, aircraft can be rendered undetectable by enemy radar [11, 12]. The manufacture of metamaterials is carried out according to user needs by designing specific unit cells to deliver desired functions [13, 14].

Several metamaterial studies use circular unit cells [13, 15, 16] as the design of the unit cells and paper as the dielectric material [13, 17, 18]. Paper is a promising material for use in electronic platform devices because it is inexpensive and environmentally friendly. Yudistira et al. [13] designed and simulated a metamaterial based on circular unit cells with paper as the dielectric to obtain a negative refractive index. The simulation achieved a high figure of merit (FoM) negative refractive index using a circular design on paper. However, they have not created a sample due to the fabrication challenges on paper.

The fabrication method is a significant issue for creating metamaterials operating at the optical and microwave spectrums. The print circuit board (PCB) method is often applied to microwave metamaterial fabrication [19, 20, 21]; however, this method is seldom used on paper. This study proposes a hand-painting method to fabricate a microwave metamaterial with a negative refractive index. Hand painting is a simple method for fabricating microwave metamaterials and is viable for use on paper, including glossy paper as used in this study. Metamaterials with a negative refractive index are widely applied to perfect lens applications. Simulation results are validated using experimental results.

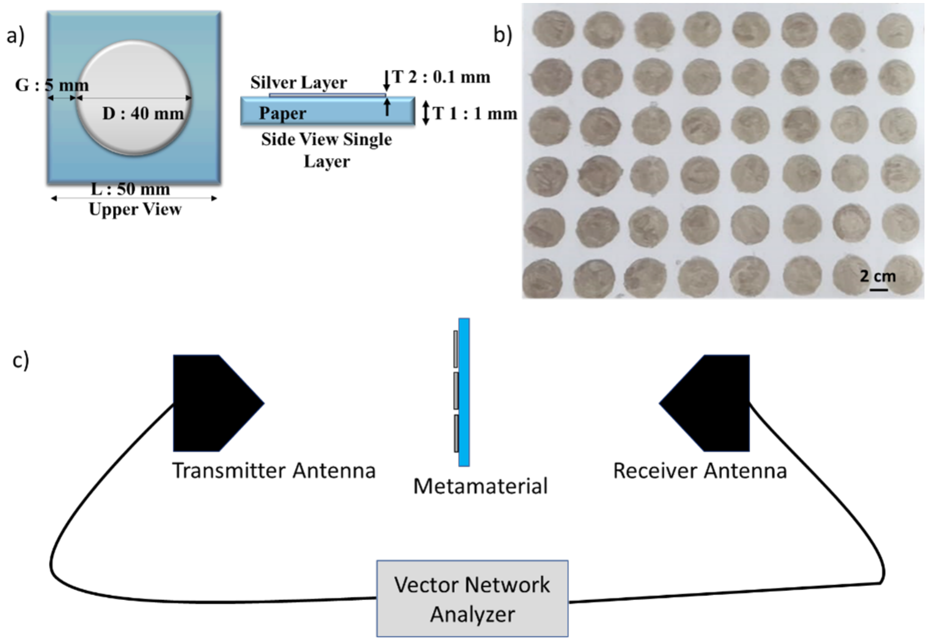

Figure 1. a) Illustration of metamaterial unit cell design, b) photograph of the metamaterial sample and c) illustration of microwave measurement set up.

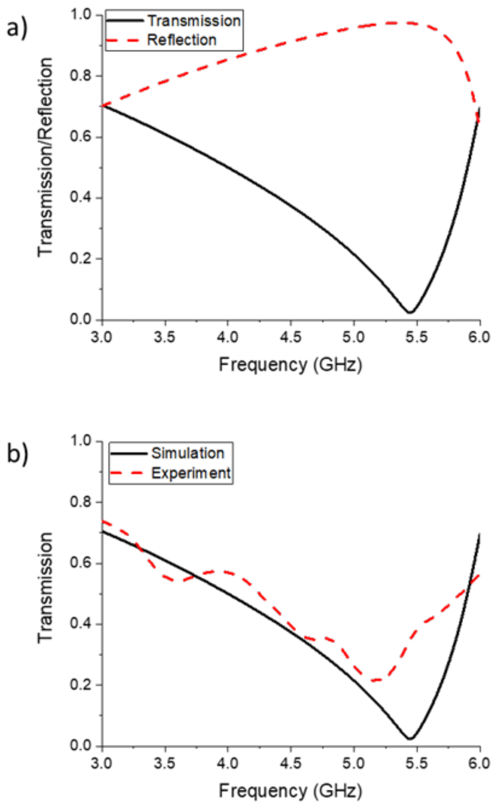

Figure 2. a) Simulation results (transmission and reflection) and b) simulation and experiment results for transmission

2. MATERIAL DESIGN, SILMULATION, AND FABRICATION PROCESS

A negative refractive index was obtained on a circular design in a previous study [13, 22]. Loop surface current existing in the surface of the circular shape produces the magnetization phenomenon, the presence of which is indicated by the permeability of the sample. The huge electric field existing in the gap between the circular shape is responsible for the polarization phenomenon, with its permittivity describing the polarization of the sample. The metamaterial design is illustrated in Figure 1a. The circular diameter (D), length of unit cell (L), unit cell gap size (2G), paper thickness (T1), and silver thickness (T2) are 40 mm, 50 mm, 10 mm, 1 mm, and 0.1mm, respectively.

Numerical simulation work employed the CST Studio Suite 2019 software, with the circular conductor model as silver and the substrate model as paper. The x-y boundary condition is described as the unit cell, and the z boundary condition is described as open (add space). The properties of silver and paper are 13,000 S/m for conductivity (conductive material), and 2.31 for relative permittivity (dielectric material), respectively. The 3 – 6 GHz frequencies are used in the simulation spectrum.

Metamaterial sample fabrication is performed using a 3D printing mold and a paintbrush by the inexpensive and straightforward hand-painting method. The first fabrication process is making a mold using a 3D printing machine. This mold is then placed onto glossy paper. A paintbrush is then used to apply the silver ink. The 3D printing cast can help the painting process achieve a perfect sample shape. When the painting process is complete, the mold is removed from the glossy paper. The fabricated metamaterial by hand painting is presented in figure 1b.

The microwave measurement system presented in figure 1c is set up to measure the fabricated metamaterial by hand painting's performance. The vector network analyzer Measall KC901V is used on the microwave measurement set up. The generated spectrum of vector network analyzer Measall KC901V can be tailored from 9 kHz to 6.8 GHz. Two Deepace R101C antennas are connected to a vector network analyzer as transmitter and receiver antennas. The range

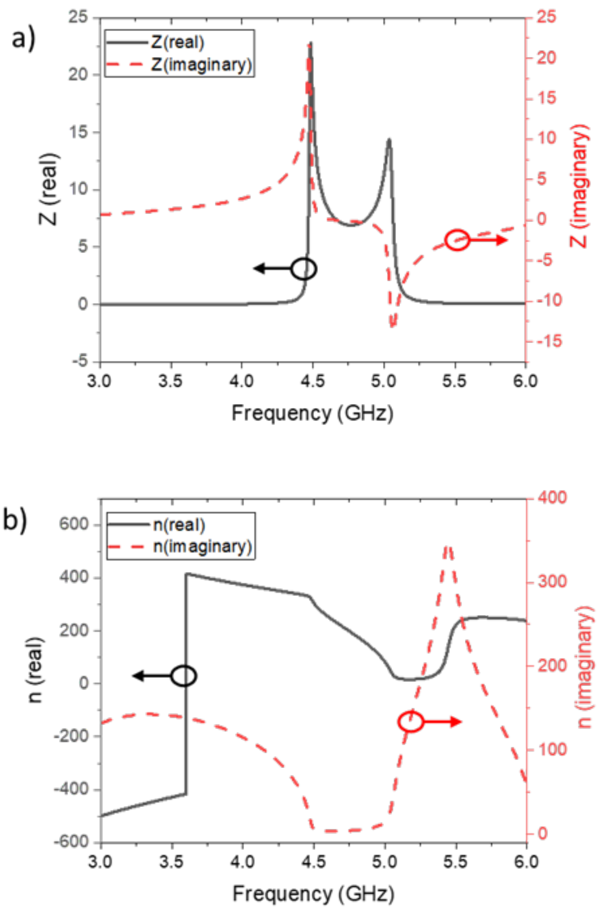

Figure 3. a) The impedance of the metamaterial and b) the refractive index of the metamaterial

frequency of the Deepace R101C antenna is 730 MHz – 6.5 GHz. Therefore, the frequency spectrum used in this experiment is similar to the simulation range of 3–6 GHz. The microwave propagates through the metamaterial. Therefore, the presented scattering parameter (S-parameter) on the vector network analyzer depends on the metamaterial's properties. The S-parameter from the experiment is used to validate the S-parameter from the simulation.

3. THE METAMATERIAL PROPERTIES PREDICTING

The reviewed S-parameters on this work are reflection (S11) and transmission (S12). The relationships between reflection (S11) and transmission (S12) and impedance (z) and refractive index (n) are described by Equations 1 and 2 [13, 23].

$$S_{11} = \frac{R_1(1 - e^{i2nk_0l})}{1 - (R_1)^2 e^{i2nk_0l}} \tag{1}$$

$$S_{12} = \frac{1 - (R_1)^2 e^{i2nk_0l}}{1 - (R_1)^2 e^{i2nk_0l}} \tag{2}$$

$$R_1 = \frac{Z - 1}{Z + 2} \tag{3}$$

where $k0$ is the wavenumbers in vacuum space and l is sample thickness, respectively. Impedance can be predicted

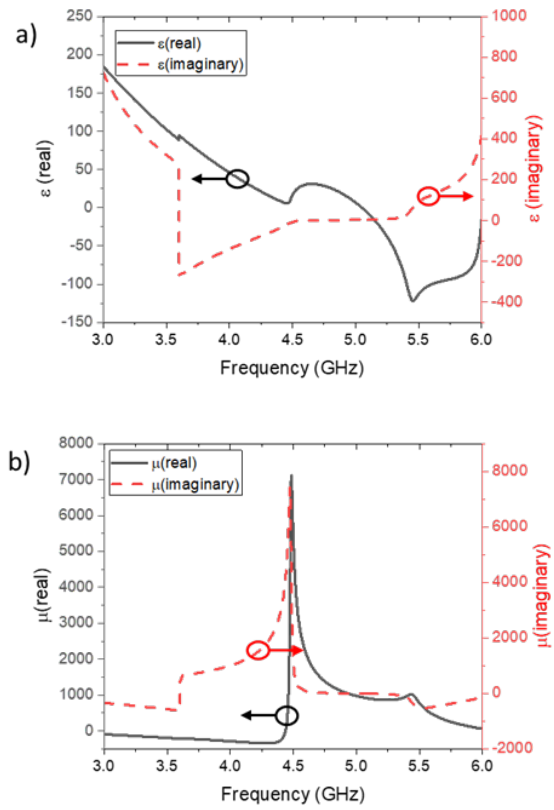

Figure 4. a) The permittivity of the metamaterial and b) the permeability of the metamaterial.

from Equations 1 and 2, as modeled in Equation 4:

$$Z = \pm\sqrt{\frac{(1 + S_{11})^2 - S_{12}^2}{(1 - S_{11})^2 - S_{12}^2}} \tag{4}$$

Calculating refractive index is similar to calculating impedance by inverting Equations 1 and 2:

$$e^{ink_0l} = X \pm \sqrt{1 - X^2} \tag{5}$$

$$X = \left(\frac{1}{2S_{12}}\right)(1 - S_{11}^2 + S_{12}^2) \tag{6}$$

A passive medium is usually applied for the metamaterial. The real impedance and the imaginary refractive index are greater than zero to describe a passive medium. The electrical properties of metamaterial are sensitive to the perturbation of the S-parameter. Therefore, the refractive index can be predicted from another equation not involved in specifying the root sign Equations 4 and 5. Equation 7 can predict the refractive index (n):

$$e^{j(\mathrm{Im}\{k_0\})} = \frac{S_{12}}{1 - S_{11}R_1} \tag{7}$$

Equation 8 and 9 are used for the estimation of permeability and permittivity.

$$\epsilon = \frac{n}{Z} \tag{8}$$

$$\mu = nZ^2 \tag{9}$$

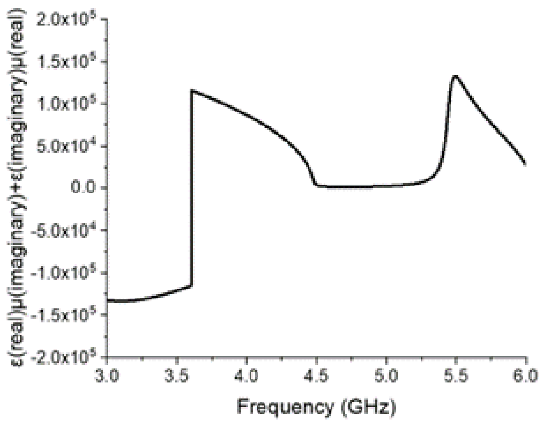

Figure 5. The calculation of ϵ(real) μ (imaginary)+ ϵ(imaginary) μ(real)

4. RESULTS AND DISCUSSION

Figure 2a presents the simulation's transmission result (black line) and reflection result (red dashed line). The peak of low transmission is 0.02286 at 5.44 GHz, and the peak of high reflection is 0.97494 at 5.38 GHz.

Discrepancies between the simulation and experiment results exist as shown in Figure 2b. The lowest peak frequency is 0.02 at 5.44 GHz for the simulation (black line) and 0.21 at 5.17 GHz for the experiment (red dashed line). The simulation shows a tendency to follow a downward pattern before rising, while the experiment shows rises and falls but still has one lowest peak frequency. The perturbation of transmission experiment results is due to existing noise during the measuring of the sample. The lowest peak frequency of the simulation is at 5.44 GHz, while the lowest peak frequency of the experiment is at 5.17 GHz. The lowest peak frequency of the simulation is close to the lowest peak frequency of the experiment. Several factors, such as the silver ink's non-uniform thickness and the imperfect circular shape of the fabricated samples, can affect the disparity between simulation data and experiment data. Overall, the experiment results have a similar trend to the simulation results.

The metamaterial impedance and refractive indexes are retrieved from Equations 4 and 7, respectively. The retrieving of metamaterial properties, such as impedance and refractive index, requires the scattering parameter results, transmission, and reflection, as in Figure 2a. Figures 3a and 3b present the impedance and refractive indexes of the metamaterial, respectively. The real impedance and imaginary refractive index have positive values at 3–6 GHz that fulfill the passive medium criteria. Refractive index with negative values is yielded at 3–3.6 GHz. High transmission performance is delivered at the spectrum of the negative refractive index. The permittivity and permeability properties are involved in the proving of refractive index with negative value performance.

Permittivity and permeability are estimated using Equations 8 and 9, respectively. Figures 4a and 4b present permittivity and permeability, respectively. The permittivity describes the polarization in the unit cell, which is mainly yielded in the tiny gap of the unit cell. Meanwhile, permeability represents the magnetization of the unit cell, produced due to its loop current. The fundamental idea of a negative refractive index condition is that the controlling unit cells simultaneously yield the negative real permittivity and the negative real permeability. However, Figure 4 presents the positive real part of the permittivity and the permeability of the negative refractive index at 3–3.6 GHz. Tung et al. [24] have introduced another basic concept for negative refractive index metamaterial conditions by stating that Equation 10 must be fulfilled to achieve negative refractive index in a metamaterial:

$$\epsilon(\text{real})\mu(\text{imaginary}) + \epsilon(\text{imaginary})\mu(\text{real}) < 0 \qquad (10)$$

Figure 5 presents the calculation of ϵ(real) μ(imaginary)+ ϵ(imaginary) μ(real) to find the spectrum which satisfies Equation 10. The calculation of ϵ(real) μ(imaginary)+ ϵ(imaginary) μ(real) is less than zero at the negative refractive index regime; thus, this regime could perform as a negative refractive index even though the real permittivity or the real permeability value is not negative. The satisfying of Equation 10 conditions is fulfilled at the negative refractive index spectrum.

5. CONCLUSION

This study successfully fabricated a negative refractive index metamaterial based on circular shape with paper as dielectric by using the hand-painting method. The limitations of the fabrication method produce the disparity between experiment and simulation results. The hand-painting method has limitations, such as the non-uniform conductive silver line thickness and the imperfect circular shape of the fabrication sample. Overall, the experiment results show a similar trend to the simulation results. The calculation of ϵ(real) μ(imaginary)+ ϵ(imaginary) μ(real) is presented to analyze the negative refractive index. The calculation of ϵ(real) μ(imaginary)+ ϵ(imaginary) μ(real) is less than zero or negative value at 3–3.6 GHz, which fulfills Equation 10.

FUNDING

The authors are grateful to the Direktorat Sumber Daya, Direktorat Jenderal Pendidikan Tinggi, Kementerian Pendidikan, Kebudayaan, Riset dan Teknologi, World Class Research Program (No. 081/E4.1/AK.04.PT/2021) for fully supporting this research

AUTHOR CONTRIBUTIONS

Mr. Hamonangan: writing the manuscript, sample fabricating, measuring, and data analysis. **Dr. Yudistira** mathematical analysis, wrote the manuscript, and managed a research project. **Ms Qalbina, Dr. Faisal and Dr. Saputro** revising the manuscript. All authors approved the final manuscript.

REFERENCES

[1] Yuandan Dong, T. Itoh, Metamaterial-Based Antennas, Proceedings of the IEEE 100 (7) (2012) 2271–2285. https://doi.org/10.1109/JPROC.2012.2187631.

[2] M. Kim, J. Rho, Metamaterials and imaging, Nano Convergence 2 (1) (2015) 22. https://doi.org/10.1186/s40580-015-0053-7.

[3] J. Pendry, Negative refraction, Contemporary Physics 45 (3) (2004) 191–202. https://doi.org/10.1080/00107510410001667434.

[4] K. Liu, R. Zhang, Y. Liu, X. Chen, K. Li, E. Pickwell-Macpherson, Gold nanoparticle enhanced detection of EGFR with a terahertz metamaterial biosensor, Biomedical Optics Express 12 (3) (2021) 1559. https://doi.org/10.1364/BOE.418859.

[5] S. Lin, X. Xu, F. Hu, Z. Chen, Y. Wang, L. Zhang, Z. Peng, D. Li, L. Zeng, Y. Chen, Z. Wang, Using Antibody Modified Terahertz Metamaterial Biosensor to Detect Concentration of Carcinoembryonic Antigen, IEEE Journal of Selected Topics in Quantum Electronics 27 (4) (2021) 1–7. https://doi.org/10.1109/JSTQE.2020.3038308.

[6] H. T. Yudistira, L. Y. Ginting, K. Kananda, High absorbance performance of symmetrical split ring resonator (SRR) terahertz metamaterial based on paper as spacer, Materials Research Express 6 (2) (2018) 025804. https://doi.org/10.1088/2053-1591/aaf27e.

[7] D. Viet, N. Hien, P. Tuong, N. Minh, P. Trang, L. Le, Y. Lee, V. Lam, Perfect absorber metamaterials: Peak, multi-peak and broadband absorption, Optics Communications 322 (2014) 209–213. https://doi.org/10.1016/j.optcom.2014.02.037.

[8] A. Palomares-Caballero, C. Molero, A. Alex-Amor, I. Parellada-Serrano, F. Gamiz, P. Padilla, J. Valenzuela-Valdes, Metamaterial-Based Reconfigurable Intelligent Surface: 3-D Meta-Atoms Controlled by Graphene Structures, preprint (Apr. 2021). https://doi.org/10.36227/techrxiv.14479290.v1.
URL https://www.techrxiv.org/doi/full/10.36227/techrxiv.14479290.v1

[9] H. Teguh Yudistira, A. Pradhipta Tenggara, V. Dat Nguyen, T. Teun Kim, F. Dian Prasetyo, C.-g. Choi, M. Choi, D. Byun, Fabrication of terahertz metamaterial with high refractive index using high-resolution electrohydrodynamic jet printing, Applied Physics Letters 103 (21) (2013) 211106. https://doi.org/10.1063/1.4832197.

[10] H. T. Yudistira, A. P. Tenggara, S. S. Oh, V. Nguyen, M. Choi, C.-g. Choi, D. Byun, High-resolution electrohydrodynamic jet printing for the direct fabrication of 3D multilayer terahertz metamaterial of high refractive index, Journal of Micromechanics and Microengineering 25 (4) (2015) 045006. https://doi.org/10.1088/0960-1317/25/4/045006.

[11] L. Yin, J. Doyhamboure-Fouquet, X. Tian, D. Li, Design and characterization of radar absorbing structure based on gradient-refractive-index metamaterials, Composites Part B: Engineering 132 (2018) 178–187. https://doi.org/10.1016/j.compositesb.2017.09.003.

[12] Hu Tao, N. I. Landy, K. Fan, A. C. Strikwerda, W. J. Padilla, R. D. Averitt, Xin Zhang, Flexible terahertz metamaterials: towards a terahertz metamaterial invisible cloak, in: 2008 IEEE International Electron Devices Meeting, IEEE, San Francisco, CA, USA, 2008, pp. 1–4. https://doi.org/10.1109/IEDM.2008.4796673.
URL http://ieeexplore.ieee.org/document/4796673/

[13] H. T. Yudistira, M. Asril, High figure of merit cylinder-shaped negative refractive index metamaterial based on paper as dielectric material, Micro & Nano Letters 16 (7) (2021) 387–391. https://doi.org/10.1049/mna2.12062.

[14] H. T. Yudistira, S. Liu, T. J. Cui, H. Zhang, Tailoring polarization and magnetization of absorbing terahertz metamaterials using a cut-wire sandwich structure, Beilstein Journal of Nanotechnology 9 (2018) 1437–1447. https://doi.org/10.3762/bjnano.9.136.

[15] T. Ramachandran, M. R. Iqbal Faruque, M. T. Islam, Left-handed Circular-Shaped Compact Metamaterial for X- and Ku-Band applications, Journal of Physics: Conference Series 1529 (5) (2020) 052021. https://doi.org/10.1088/1742-6596/1529/5/052021.

[16] O. B. Ayop, M. K. Abd Rahim, N. A. Murad, N. A. Samsuri, R. Dewan, TRIPLE BAND CIRCULAR RING-SHAPED METAMATERIAL ABSORBER FOR X-BAND APPLICATIONS, Progress In Electromagnetics Research M 39 (2014) 65–75. https://doi.org/10.2528/PIERM14052402.

[17] H. Tao, L. R. Chieffo, M. A. Brenckle, S. M. Siebert, M. Liu, A. C. Strikwerda, K. Fan, D. L. Kaplan, X. Zhang, R. D. Averitt, F. G. Omenetto, Metamaterials on Paper as a Sensing Platform, Advanced Materials 23 (28) (2011) 3197–3201. https://doi.org/10.1002/adma.201100163.

[18] A. Sadeqi, H. R. Nejad, S. Sonkusale, Low-cost metamaterial-on-paper chemical sensor, Optics Express 25 (14) (2017) 16092. https://doi.org/10.1364/OE.25.016092.

[19] Y. J. Kim, J. S. Hwang, Y. J. Yoo, B. X. Khuyen, J. Y. Rhee, X. Chen, Y. Lee, Ultrathin microwave metamaterial absorber utilizing embedded resistors, Journal of Physics D: Applied Physics 50 (40) (2017) 405110. https://doi.org/10.1088/1361-6463/aa82f4.

[20] E. L. Chuma, Y. Iano, G. Fontgalland, L. L. B. Roger, H. Loschi, PCB-integrated non-destructive microwave sensor for liquid dielectric spectroscopy based on planar metamaterial resonator, Sensors and Actuators A: Physical 312 (2020) 112112. https://doi.org/10.1016/j.sna.2020.112112.

[21] P. Zuo, T. Li, M. Wang, H. Zheng, E.-P. Li, Miniaturized Polarization Insensitive Metamaterial Absorber Applied on EMI Suppression, IEEE Access 8 (2020) 6583–6590. https://doi.org/10.1109/ACCESS.2019.2957308.

[22] A. Rasad, H. T. Yudistira, F. Qalbina, A. G. Saputro, A. Faisal, Multilayer flexible metamaterials based on circular shape with negative refractive index at microwave spectrum, Sensors and Actuators A: Physical 332 (2021) 113208. https://doi.org/10.1016/j.sna.2021.113208.

[23] X. Chen, T. M. Grzegorczyk, B.-I. Wu, J. Pacheco, J. A. Kong, Robust method to retrieve the constitutive effective parameters of metamaterials, Physical Review E 70 (1) (2004) 016608. https://doi.org/10.1103/PhysRevE.70.016608.

[24] N. T. Tung, V. D. Lam, J. W. Park, M. H. Cho, J. Y. Rhee, W. H. Jang, Y. P. Lee, Single- and double-negative refractive indices of combined metamaterial structure, Journal of Applied Physics 106 (5) (2009) 053109. https://doi.org/10.1063/1.3213097.

